Properties and High Temperature Dry Sliding Wear Behavior of Boronized Inconel 718

ALİ GÜNEN

Silicide-free boride layers were grown on Inconel 718 Ni-based superalloy surface at 850 °C, 950 °C, and 1050 °C for 2, 4, 6 hour by the powder pack-boronizing process using nano-sized B_4C powders. The coatings were examined using optical microscopy, scanning electron microscopy, energy dispersive spectroscopy, X-ray diffractometry, 3D profilometry, and microhardness measurements. Wear experiments were carried out on untreated and boronized Inconel 718 using a ball-on-disk tribometer under dry sliding conditions at temperatures of 25 °C, 400 °C, and 750 °C. An increase in boronizing temperature and duration increased the thickness and hardness of the obtained boride layers, which resulted in low coefficient of friction values and decreased wear rates. Scanning electron microscopy images of the worn surfaces revealed two-body abrasion as the effective wear mechanism in the untreated samples, and three-body abrasion assisted by microcracking and spalling as the dominant wear mechanism in the boronized samples. A transition from mild to severe wear occurred in the untreated samples, while wear rates remained low in the boronized samples up to 750 °C. In conclusion, boronized Inconel 718 was capable of sustaining its boride layers under 5 N for 1800 m at wear-test temperatures up to 750 °C.

https://doi.org/10.1007/s11661-019-05577-3

I. INTRODUCTION

Ni-BASED superalloys are indispensable materials for high-temperature and oxidizing environments because they can retain their mechanical properties and corrosion resistance at elevated temperatures.[1] Inconel 718 is a widely-used precipitation strengthening Ni-based superalloy with excellent tensile, fatigue, and creep strength. It is also known for its good weldability and outstanding resistance to post-weld cracking.[1,2] The combination of these properties have made Inconel 718 suitable for use in a number of applications including nuclear reactors, liquid-fueled rockets, pumps and blisks, casings and various formed sheet metal parts for aircraft and rings, turbine blades, land-based gas turbine engines, power generation units, extrusion dies, and containers and cryogenic storage, with service temperatures ranging from − 250 °C to 700 °C.[2–5]

Despite its unique combination of properties and widespread use, the wear characteristics of Inconel 718 (and many other superalloys) are often considered unsatisfactory,[6–8] especially at elevated temperatures. When used in aggressive wear environments, Inconel 718 must be coated to improve its lifetime.[9] Thermochemical coatings are a good option for achieving this requirement, many of which are capable of maintaining surface stability and mechanical properties up to 1000 °C.[10,11]

Boronizing is a thermochemical process in which boron atoms with small atomic radius diffuse from the surface into the interior of the material at high temperatures to form hard boride layers. Boronizing is somewhat unique compared to other thermochemical processes as it generally provides harder coatings on steel and superalloys in comparison to other thermochemical coating processes such as nitriding, titanizing, chromizing *etc*.[8,12–14] It should be noted, however, that the boronizing of pure Ni and Ni-based alloys requires the use of Si-free boronizing powders. Otherwise, the formation of silicides or borosilicides in boride layers is inevitable. This is particularly undesirable for wear applications, due to the inherent porosity and low hardness of the resulting borosilicide layers.[7,9,15] It has been stated that the topmost silicide layer that forms with the use of Si-containing boronizing media has a hardness of only ~ 500 HV, and that it must be removed from the surface to eliminate its detrimental effects on wear resistance.[7,16,17] However, in recent years it has been found that silicide-free boride layers can be grown on Ni-based superalloys[18–20] using proprietary/

ALİ GÜNEN is with the Iskenderun Technical University, Faculty of Engineering and Natural Sciences, Metallurgy and Materials Engineering Department, 31200 Hatay, Turkey. Contact e-mail: ali.gunen@iste.edu.tr

Manuscript submitted April 19, 2019.
Article published online December 6, 2019

specialized SiC-free boronizing media such as Ekabor-Ni or by substituting the SiC filler with B_4C.

When considering boronized Ni-based superalloys, there are only few studies focused on the friction and wear behavior of these superalloys. Dinc *et al.*[7] boronized Inconel 718 at 900 °C for durations ranging from 2 to 12 hour using Si-containing Ekabor II powders, and investigated the friction and wear properties of the boronized alloys under dry sliding conditions at room temperature. Boronizing led to improvements in wear resistance, and the highest wear resistance was found in the sample that boronized for 4 hour. Wear resistance decreased when the boronizing duration was further increased to 8 and 12 hour; this was based on the increase in residual stresses within the silicide layer. Deng *et al.*[17] boronized Inconel 718 at 980 °C for 10 hour using paste boronizing and investigated the effects of aging on friction and wear behavior at room temperature. They reported that the wear resistance was improved by the boronizing treatment, and that it could be improved even further with aging treatments. Günen and Kanca[18] boronized Inconel 625 with three different powders, and investigated the layers grown on the surfaces using X-ray diffraction (XRD) and microhardness tests. They stated that nanoboron and hexagonal boron nitride powders could be an alternative to commercial Ekabor-Ni. Petrova *et al.*[19] investigated the wear, corrosion and oxidation resistance of boronized Inconel 625. They concluded that boronizing improved corrosion and wear resistance at room temperature as well as high-temperature oxidation resistance. Campos-Silva *et al.*[20] investigated the boride layers developed on Inconel 718 using optical microscopy (OM), XRD, energy dispersive spectroscopy (EDS), scratch tests, and indentation experiments. They claimed that the adhesion of the boride layers on the substrate depended on hardness, residual stress, Young's modulus and applied load.

In regard to coating studies performed on Inconel 718 using methods other than boronizing, Döleker *et al.*[21] coated Inconel 718 with YSZ/Gd2Zr_2O_7 ceramics by Electron-beam physical vapor deposition (EB-PVD) technique and investigated the oxidation resistance of untreated and coated samples in open air at 1000 °C for 8, 24 and 100 hour. They found that the coated Inconel 718 exhibited better oxidation resistance and also that the Inconel 718 alloy was not suitable for longer treatment duration at 1000 °C.[21] Kumar *et al.*[22] examined the effects of aluminizing and ultrasonic shot peening processes (USSP) on the hot corrosion resistance of Inconel 718 in NaCl (100 wt pct) and Na_2SO_4 (75 wt pct) + NaCl (15 wt pct) + V_2O_5 (10 wt pct) at 700 °C. They found that the aluminizing process improved the corrosion resistance by 50 pct, mainly because of the formation of a uniform alumina layer which acted as a barrier. Whereas, USSP decreased the wear resistance by 2 times, which could be explained by the increase in surface activity of the alloying elements.[22] Feng *et al.*[23] investigated high-temperature wear behavior of laser cladded and shielded metal arc welded Inconel 625 at both room temperature and elevated temperatures (550 °C, 600 °C, and 650 °C). They found that the laser cladded samples showed higher wear resistance due to the higher hardness and lower dilution of iron.

Many surface treatments such as boronizing have been developed to improve the wear performance of Ni-based superalloys. Only few studies have focused on identifying the wear mechanisms involved in the high-temperature wear behavior of boronized Ni-based superalloys. The aim of this work is to investigate the dry sliding high-temperature (25 °C, 400 °C, 750 °C) friction and wear behavior of free-silicide boride layers grown on the surfaces of an Inconel 718 superalloy by utilizing a ball-on-disk type wear rig at a normal load of 5 N and sliding velocity of 0.6 m/s. The operative wear mechanisms of the worn surfaces of both the boride layers and abrasive ball have been analyzed by scanning electron microscopy, energy dispersive spectroscopy, and 3D profilometry.

II. MATERIALS AND METHODS

Inconel 718 type Ni-based superalloy was used as the substrate material for the boronizing process. In the acquisition catalog of Inconel 718, it is stated that AMS 5596 heat treatment is applied to Inconel 718 sheet plate. This heat treatment can be summarized as follows: solution anneal at 925 °C to 1010 °C followed by rapid cooling (water), precipitation hardening at ~ 20 °C for 8 hour, furnace cooling to ~ 620 °C, holding at 620 °C for a total aging time of 18 hour, followed by air cooling. A Thermo Scientific—iCAP™ 7400—ICP-OES Spectrophotometric atomic emission (ICP) analyzer was used for chemical analysis of Inconel 718 samples. The chemical composition of Inconel 718 in mass percent are as follows: 54.5 wt pct Ni, 20.1 wt pct Cr, 12.5 wt pct Fe, 5.5 wt pct Nb, 2.8 wt pct Mo, 1.05 wt pct Ti, 0.5 wt pct Al, and 3.5 wt pct other balance elements.

Before boronizing, all samples were cut to a size of $50 \times 50 \times 3$ mm^3 using a guillotine shear. Sample surfaces to be coated were then ground using SiC papers (600 to 1500 grit) to remove undesirable substances such as oil and oxide residues and also to obtain smoother surfaces. After grinding, the samples were rinsed in distilled water, and then ultrasonically cleaned in acetone for 15 minutes.

The boronizing treatment was carried out at 850 °C, 950 °C, and 1050 °C for 2, 4 and 6 hours (Table I). Details of the boronizing process can be found in previous work.[8] Each sample was placed into a hermetically sealed stainless steel container packed with the boronizing powders containing 90 wt pct nano-sized B_4C and 10 wt pct KBF_4. Concerning silicide formation, 2 cm only Al_2O_3 powder was added to the top of the boron powder mixture instead of SiC which is used for boronizing of steels to prevent oxidation. Sealing of the container was done in a glove box under argon. The sealed container was then placed into an electrical resistance furnace which was heated to the boronizing temperature under atmospheric conditions. After the boronizing step the container was removed from the furnace and cooled to room temperature in air. In order

to increase the diffusion rate in boronizing process, B_4C boron powders with size of 50 to 100 nm were used in the study.

Metallography, microhardness and XRD specimens with $10 \times 10 \times 3$ mm^3 size were obtained from the boronized $50 \times 50 \times 3$ mm^3 specimens using a precision cutting device. The cross-sections of the specimens were hot mounted, ground with SiC papers (320 to 1500 grit) and then polished with diamond paste (1 μm and 0.25 μm) to obtain mirror finish. After polishing, the samples were electro-etched in a solution of 70 mL H_3PO_4 and 30 mL water at 5 V for 60 seconds to reveal microstructural details.

Optical studies were carried out using a Nikon MA-100 optical microscope equipped with Clemex Vision image analysis software. Scanning electron microscopy (SEM) studies were conducted using a TESCAN S8000 BrightBeam^{TM} field emission scanning electron microscope equipped with EDS capability, operating at 25 kV accelerating voltage.

Microhardness tests of the obtained boride layers were performed using a QNESS Q10 hardness tester with a Vickers pyramid indenter using 100 gf load and 15-seconds dwell time according to the ASTM-E384. Each hardness value was the average of 5 measurements. The thicknesses of the boride layers were determined by a Clemex digital thickness measurement instrument attached to the optical microscope. The hardness and thickness values were given based on the average of 10 measurements taken from the cross section of the boride layer. The surface roughness of the specimens was measured using a Hommelwerke T8000 stylus profilometer. The stylus tip was set to trace along 4 mm at a speed of 2 mm/s. XRD analyses were carried out using a computer-controlled Rigaku SmartLabTM with Cu Kα radiation (λCu = 0.1540 nm) and 2θ angles ranging from 5 to 90 deg and integration time of 280 seconds.

Since Inconel 718 has been reported to maintain its mechanical stability from room temperature to 650 °C,[16,20,21] wear-test temperatures were chosen as 25 °C (room temperature), 400 °C, and 750 °C. 750 °C was used in one study performed on Inconel 617, Stellite 6 alloys and X32CrMoV33 hot work tool steel by Birol[24] who determined that due to its inferior oxidation resistance X32CrMoV33 degraded rapidly while Inconel 617 and Stellite 6 alloys not owing to protective oxides that sustain the abrasion without spalling. Dry sliding wear tests of untreated and boronized Inconel 718 were carried out under 5 N load with a sliding velocity of 0.6 m/s for 30 minutes against a WC abrasive ball (hardness 1917 HV) with 6 mm diameter at 25 °C, 400 °C, and 750 °C on a ball-on-disk type TURKYUS POD&HT&WT (Turkey) wear tester. Heat input was provided by the electric resistors within the integrated heating cabinet (furnace) and the temperature was held constant using K-type thermocouple. Three samples were tested for each experimental condition and the results averaged. The weight of the abrasive ball was measured after each test.

Table I. Summary of Uncoated and Boronized Samples Treated at Various Temperatures and Durations

Sample	Boronizing Process	
Naming	Temperature (°C)	Duration (h)
850-2	850	2
850-4	850	4
850-6	850	6
950-2	950	2
950-4	950	4
950-6	950	6
1050-2	1050	2
1050-4	1050	4
1050-6	1050	6
I-718	untreated	untreated

At the end of the wear tests, cross-sectional imaging was done using a 3D profilometer along 4 different paths across the circular wear track to estimate the volumetric wear losses of the samples. The wear track cross section was considered as a half ellipse. The formulas used in the calculation of wear losses are given below.

$$L = 2\pi r \quad [1]$$

$$V = 0.25\pi WD \quad [2]$$

$$Wr = V/FS \quad [3]$$

where L Length of wear track (mm), V Wear track volume (mm^3), r Radius of wear track (mm) W Average wear track width (μm), D Average wear track depth (μm), F Test load (N), S Sliding distance (m), and Wr Wear rate (mm^3/Nm).

III. RESULTS AND DISCUSSION

A. *Microstructure and XRD Analyses*

Figure 1 shows a cross-section OM image of untreated Inconel 718 and cross-section SEM images of Inconel 718 samples boronized at the temperatures 850 °C, 950 °C, and 1050 °C for 4 hour.

A coating layer with a toothless morphology was grown as a result of boronizing process (Figure 1). Boride layers with this morphology has been verified and reported in previous studies conducted on superalloys[8,17,20] and high alloy steels.[25–27] The microstructure consists of 3 regions: the boride layer, the diffusion zone, and the matrix. It is noteworthy that the diffusion layer is fairly narrow, compared to that observed in most steels. This difference can be attributed to the composition of Inconel 718 superalloy, which reduces boron diffusion towards the interior when compared to steels. This resulted in the thinning of the coating layer and diffusion zone. When boronizing time and temperature were increased, the thickness and hardness of the coatings increased (Figure 1 and Table II).

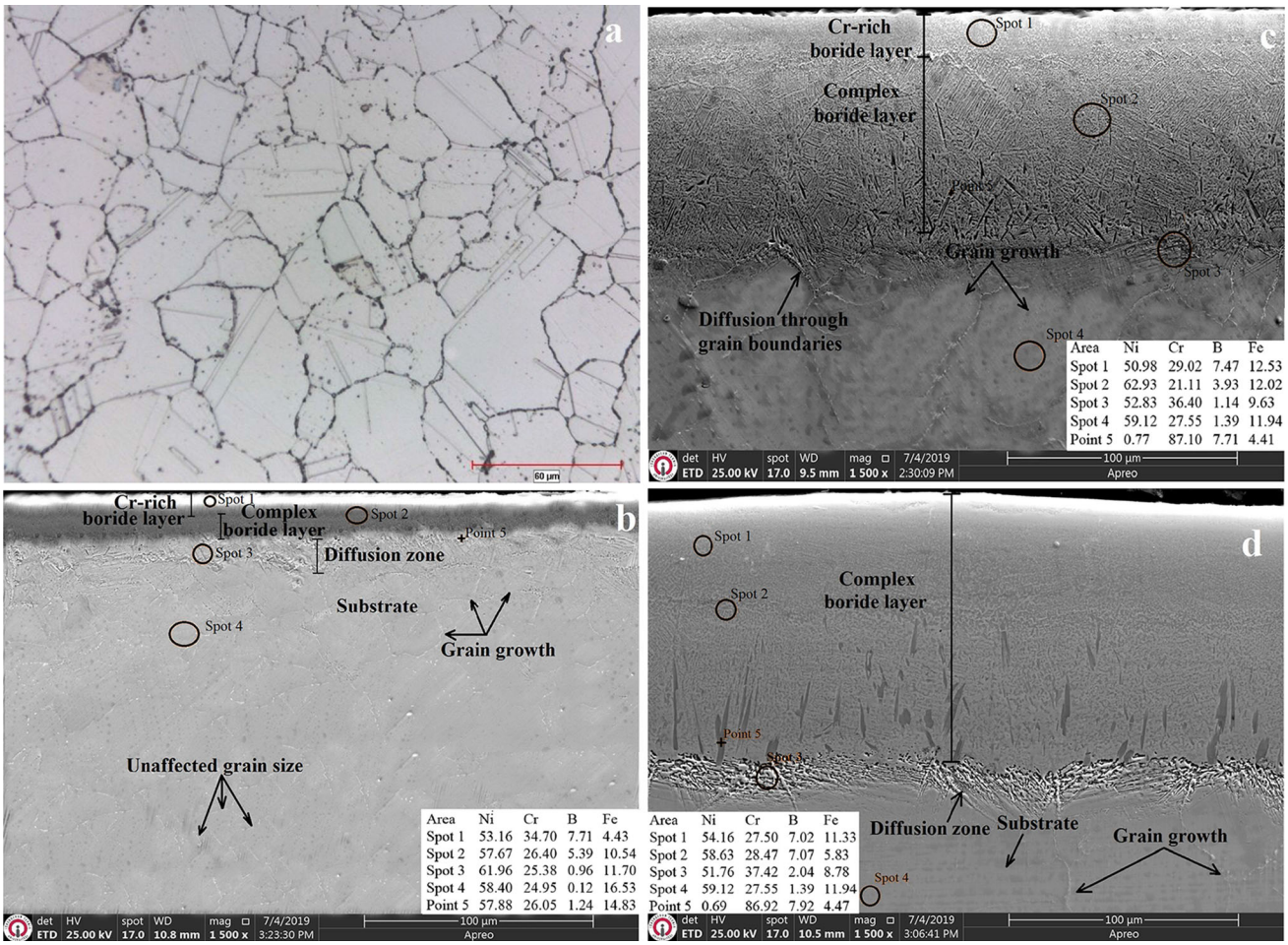

Fig. 1—Cross-section OM of untreated Incone1 718 (*a*), and SEM micrographs of Inconel 718 boronized for 4 h at 850 °C (*b*), 950 °C (*c*), and 1050 °C (*d*), respectively. EDS spots are marked in the relevant images.

When the morphology of the coating is examined, it exhibited a double-layered structure at 850 °C and 950 °C, (Figures 1(b) and (c)) while a more compact single layer is formed at 1050 °C (Figure 1(d)). The thickness of the Cr-rich layer increased due to increasing boronizing temperature and time. The boundary separating the two layers, which was clearly observed in 850-4 and 950-4 samples, is absent in the 1050-4 sample. The high concentration of Cr in the single layer was determined by EDS analysis. Günen and Kanca[18] found that the upper part of this double-phase layer had a higher Cr content which was also confirmed by SEM-EDS analysis in the present study. EDS spot analysis carried out using various locations on the cross section of samples (Figures 1(b) through (d)), which indicated that Cr and B decreased while Ni increased from the surface of the coating towards the interior. The reduction of Cr shown in Figures 1(c) and (d) could be explained by the formation of Cr-B islets (shown as point 5) which contained over 85 pct Cr and 7 pct boron and less than 1 pct Ni. To better understand elemental distribution patterns, EDS mapping was also performed on the cross-sectional surface of the sample boronized at 950 °C for 6 hour (950-6) (Figure 2(a)). Cr was located more at the outer layer than inner layer. Also, increase

Table II. Hardness, Thickness, and Surface Roughness of the Boride Coatings

	Coating layer		Surface Roughness	
Sample	Thickness (μm)	Hardness ($HV_{0.1}$)	Ra (μm)	Rz (μm)
850-2	20.7	2330.4	0.45	1.25
850-4	21.6	2342.5	0.59	1.57
850-6	26.5	2354.6	0.74	2.03
950-2	36.2	2378.5	0.65	1.98
950-4	69.2	2392.1	0.85	2.47
950-6	72.1	2395.8	1.01	3.02
1050-2	53.1	2405.6	0.89	2.58
1050-4	105.6	2481.7	1.02	3.18
1050-6	130.1	2587.9	1.07	3.21
I-718	—	230 to 240	0.25	0.4

Fig. 2—Elemental EDS maps of Inconel 718 treated at 950 °C for 6 h (950-6) (*a*), XRD patterns of Inconel 718 boronized at the temperatures of 850 °C, 950 °C, and 1050 °C for 4 h and untreated Inconel 718 (*b*) change hardness values of untreated and boronized Inconel 718 from surface to matrix (*c*).

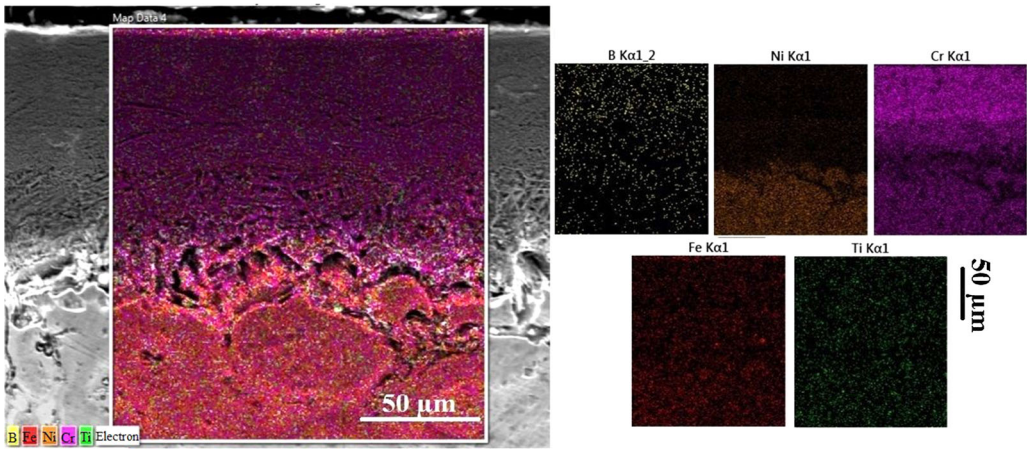
Map Data 4
50 μm
B Kα1_2
Ni Kα1
Cr Kα1
Fe Kα1
Ti Kα1
50 μm
B Fe Ni Cr Ti Electron

(a)

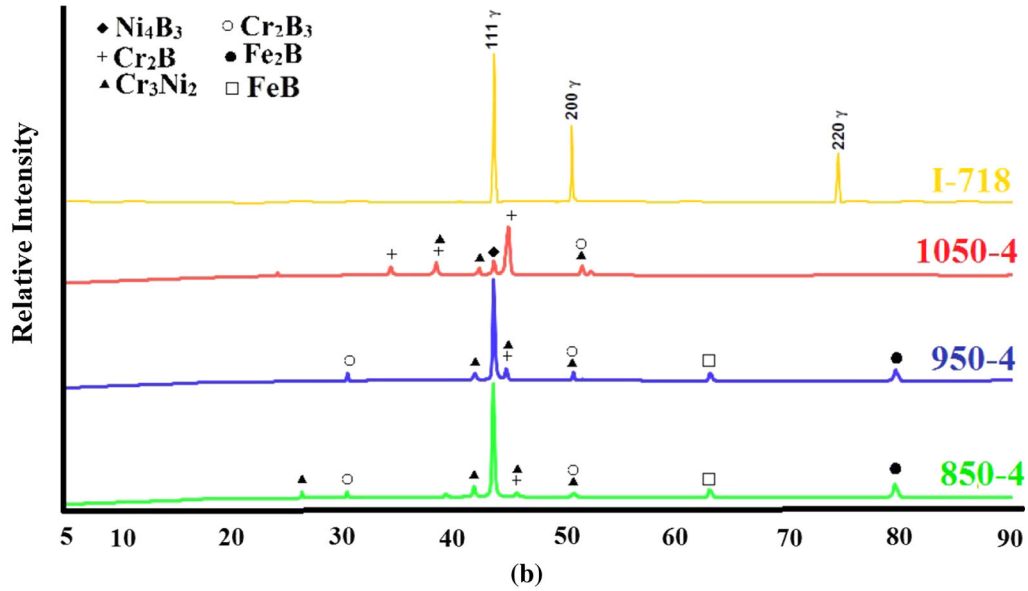
Ni4B3
Cr2B
Cr3Ni2
Cr2B3
Fe2B
FeB
111 γ
200 γ
220 γ
I-718
1050-4
950-4
850-4
Relative Intensity
5
10
20
30
40
50
60
70
80
90

(b)

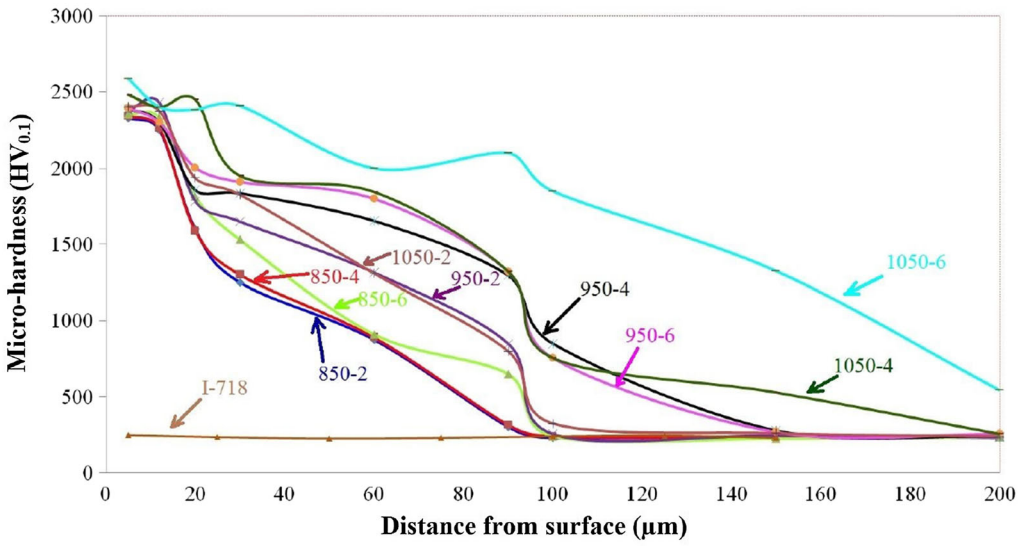
Micro-hardness (HV0.1)
Distance from surface (μm)
0
500
1000
1500
2000
2500
3000
0
20
40
60
80
100
120
140
160
180
200
1050-6
1050-2
850-4
950-2
950-4
850-6
950-6
1050-4
850-2
I-718

(c)

in Cr concentration moving from the diffusion zone (beneath the coating layer) to the boride layer is clearly observable. Similar findings were reported by Ozdemir *et al.*[27] for boronized AISI 316. They observed that Cr was concentrated at the boride layer while Ni and Fe mostly remained at the substrate. However, when boronizing temperature is increased to 1050 °C, the Cr-rich upper layer (Figure 1(c), Spot 1) shows an increased mixing tendency with the Ni-rich lower layer (Figure 1(d), Spot 1). Therefore, the double boride layer, which was apparent in samples borided at 850 °C and 950 °C (Figures 1(b) and (c)), is replaced with a complex boride layer (Figures 1(d) and 2(a)) in samples borided at 1050 °C. Grain growth and the appearance of annealing twins are also evident in the boronized samples (Figures 1(c) and (d)); however, grain growth did not occur over the entire structure and only covered a distance of 50 to 100 mm beneath the diffusion zone.

The thickness, microhardness and surface roughness values of the boride layers increased with increasing boronizing temperature and time (Table II).

Thicker boride layers were obtained in the current study than previous studies[7,17–20]; this was mainly caused by the use of nano-sized powders. The use of nano-sized powders increases the surface area of boronizing powders, which promotes higher boron potential. Thus, the diffusion can occur with lower activation energy,[28] allowing the formation of boride layers with greater thickness. The measured maximum hardness values on the surfaces of the boronized samples ranged from 2330.4 to 2587.9 $HV_{0.1}$ depending on boronizing conditions, and the hardness decreased from surface to the interior (Figure 2(c)). The hardness values are consistent with the hardness values of predominant phases (Ni_3B_4, Cr_2B) and other minor phases (Cr_3Ni_2, Cr_2B_3, FeB, Fe_2B). These phases were detected by XRD analysis (Figure 2(b)) and their hardness values were compared with the literature.[7–9,17–20] It was seen that the dominant phases changed from NixBy to CrxBy with increasing boronizing temperature. Due to the high alloy content of Inconel materials, the formation of multiple phases at different temperatures and boronizing times has been observed. This was also supported by different proportions of elements such as Ni, Cr, B, Fe, which were determined in the EDS analysis taken from the surface of the coating layer towards the interior. It is important to note that XRD analysis revealed no evidence of silicide or borosilicide formation owing to the use of proprietary/specialized SiC-free boronizing media. The formation of silicide or borosiliside phases in the boride layers is one of the major problems for wear applications. The hardness of topmost silicide phases (< 500 HV) is lower than that of nickel boride (1600 to 2000 HV) layer, and often impair the wear performance of Ni-based alloys.[17] On the other hand, only γ (austenite) phase which corresponds to face-centered cubic Ni-based γ-phase detected on untreated Inconel 718 super alloy. On the other hand, values of surface roughness (Ra and Rz) increased with increasing boronizing temperature and duration time. The increase in surface roughness may be caused by unreacted crystaline structures of boronizing powder during the boronizing process.

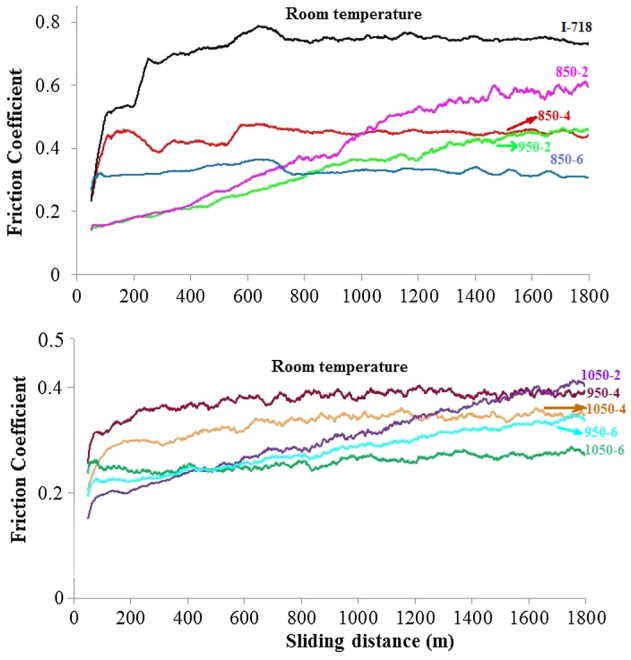

Fig. 3—COF of untreated and boronized Inconel 718 at room temperature under 5 N load.

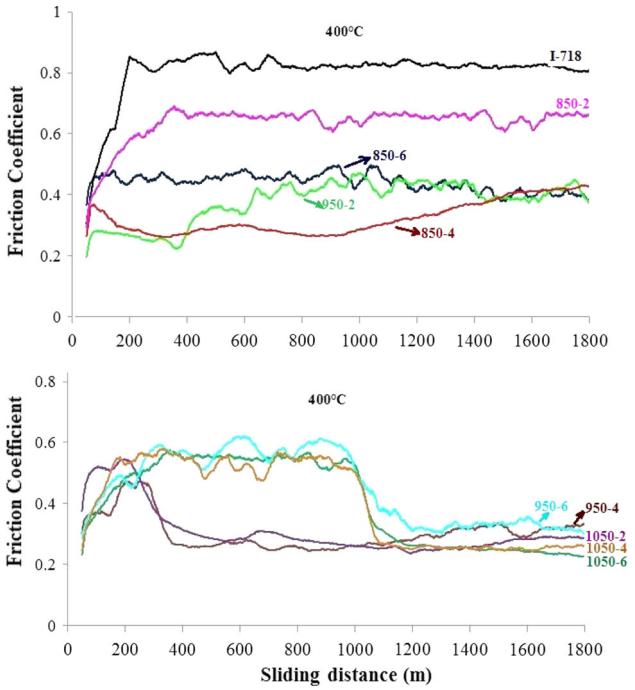

Fig. 4—COF of untreated and boronized Inconel 718 at 400 °C under 5 N load.

B. *Friction and Wear*

Engineering materials may often exhibit different wear behaviors at elevated temperatures compared to their behaviors at room temperature. Because of the high-temperature effects, it is inevitable that the mechanical strength of materials decreases and surface conditions change. As a result, the service life and/or performance of the materials may deteriorate and economic losses may occur.[29,30]

Figures 3, 4 and 5 show the COF graphs recorded during the wear tests of the untreated and boronized samples, which were carried out under 5 N at 25 °C, 400 °C, and 750 °C, respectively.

The COFs of the untreated sample were higher than those of the boronized samples at all three test temperatures. This could be attributed to severe surface damage occurring as a result of low surface hardness.[31] Also, as a result of temperature increase, an increase in both of the values and fluctuations in COF can be seen in the plots. Two reasons can be given for these effects: the first is that the different boride phases resulting from the boronizing process have different responses to temperature rise,[32] and the second is that oxide layers formed on the surface (due to the fact that the experiments were performed in air) and the spalling of these oxide layers occur during the wear tests.[11,31,33] At the beginning, the asperities resulted from different thermal expansions of phases and fracture of oxides limited the sliding speed and change the applied stress on the worn surface and this may have caused a change in the wear mechanism from two-body to three-body abrasion.[30]

On the other hand, the COF generally tends to decrease as the boronizing time and duration is increased (Figures 3, 4, and 5). In samples with low coating thickness (850-2, 850-4, 950-2), the COF shows an increasing trend over time in general sense. While in samples with high coating thickness (950-6, 1050-4, 1050-6), the COF initially shows an increase (until the roughness of the surface was removed) followed by a decrease (Figure 4). The continuous increase in COF in samples with low coating thickness could be explained by the spalling of the thin boride layer. The spalled layer may serve as an abrasive in the rest of test and thus

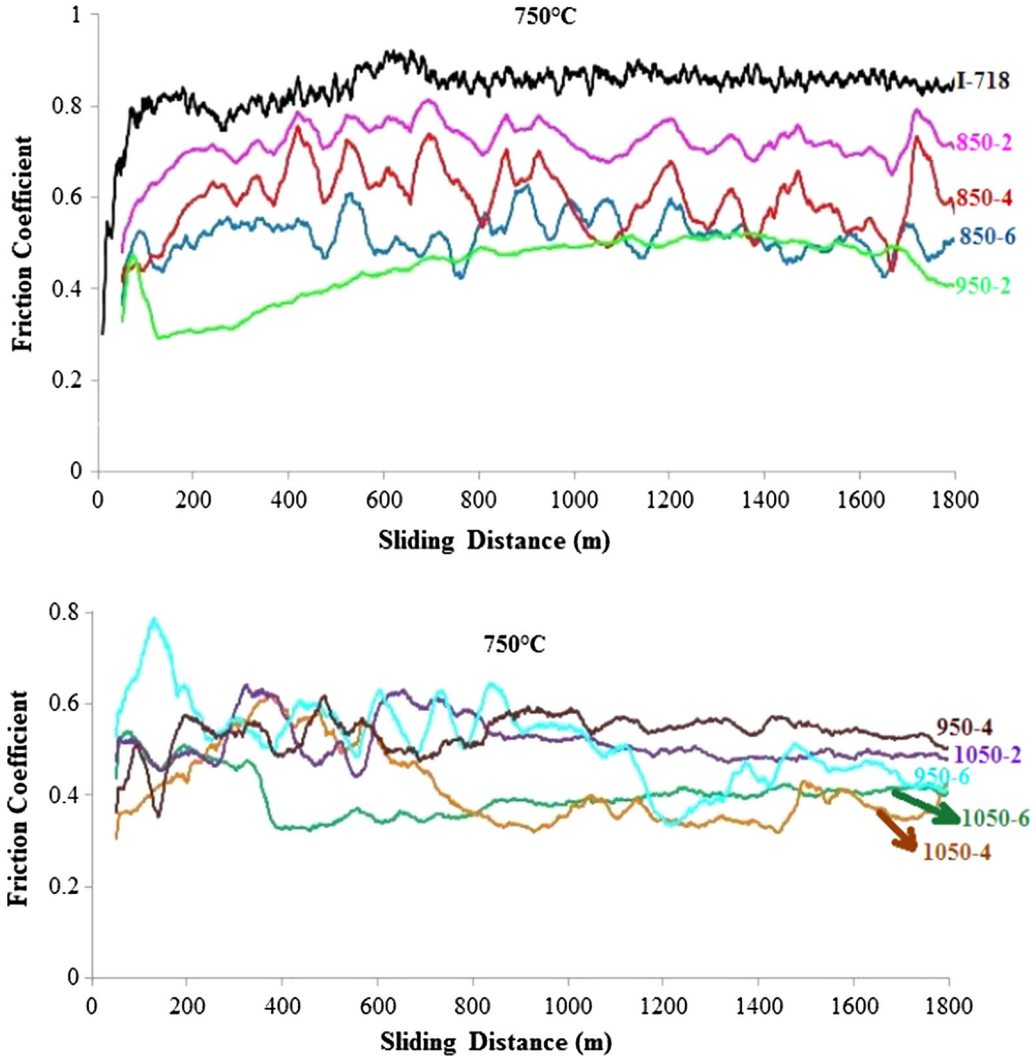

Fig. 5—COF of untreated and boronized Inconel 718 at 750 °C under 5 N.

cause more wear on the surfaces.[11] Whereas if the thickness of the hard boride layer is sufficient, the surfaces will have less roughness, a resulting lower COF and less wear will occur.

The volume losses of the untreated and boronized Inconel 718 samples wear-tested at different temperatures are given in Figure 6. Table III was also prepared for better interpretation of wear volumes and average friction coefficient values.

As seen from Figure 6 and Table III, the volume losses of boronized Inconel 718 generally decreases with increasing boronizing temperature and time. This is related to the thickness of the boride layers obtained. In the boronizing process carried out at 850 °C, the obtained maximum thickness and hardness of the boride layer was 20 μm and 2330 HV, respectively. However, coatings with thickness values exceeding 130 μm and the hardness values reaching up to 2587 HV were obtained in the samples boronized at 1050 °C for 6 hour (Table II). The hardness and thickness of the boride layers formed on the surface can have a significant effect on wear resistance.[8,32] An increase in hardness and thickness will provide more resistance to three-body and two-body abrasion, and the surface more will be more resistant to the generated wear debris.[34] In three-body wear, the penetration depth of the abrasive particles will be much less in the presence of hard boride layers and this will consequently lead to a decrease in volume losses

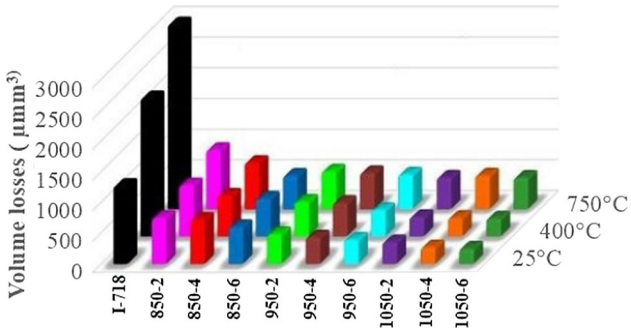

Fig. 6—Wear losses of the untreated and boronized Inconel 718 alloy, obtained at different test temperatures.

(Figure 7). As for two-body abrasive type wear, particles penetrating the surface can also plow the surface when a tangential force is applied. If the hardness of the material is increased, it also exhibits more resistance to plowing.[8,34] In Figure 7 it is also apparent that due to the existence of the hard borides the wear tracks on the boronized specimens are shallow and uneven, while the wear tracks on the untreated alloy are deeper and more uniform. The abrasive WC ball abraded the softer untreated surface more easily and homogeneously, whereas the borided surfaces containing hard borides showed greater resistance to abrasion.[35] This is clearly seen from the peaks and troughs in the 3D profilometer views (Figures 7(d) through (f)). The surface roughness decreased with increasing wear-test temperature. At elevated temperatures, the COF decreases due to the formation of oxide layer on the surfaces and the thermal expansion difference between different grown phases decreases. This result is corroborated with the wear-test results of Figure 6. All coated samples show higher wear resistance under all wear-test conditions, and the cumulative volume losses of the boronized samples at 25 °C, 400 °C, and 750 °C were about 5.5, 9.1, and 6.4 times less than untreated Inconel 718, respectively.

SEM images of the worn surfaces were examined to further understand the operative wear mechanisms. Figures 8, 9 and 10 show the SEM views obtained from the surfaces of untreated I-718, 850-2, and 1050-6 after wear testing performed at 25 °C, 400 °C, and 750 °C, respectively.

Considering the worn surfaces of untreated Inconel 718 (I-718) show clear signs of microcutting and two-body abrasion under all wear conditions (Figure 8). The width and depth of the wear grooves increase with increasing temperature. Signs of plastic deformation such as plowing and ridge formation appear on samples worn at elevated temperatures (400 °C and 750 °C). The wear mechanism is abrasive wear at all three temperatures, but a transition from cutting to plowing takes place between room temperature (25 °C) and 400 °C. The softening of Inconel 718 allows more plastic deformation to occur, causing plowing and ridge formation to dominate at higher temperatures. Thus, the effective wear mechanism for

Table III. The Average Coefficient of Friction and Volume Losses Obtained from Wear Tests

	Mean Values of COF			Volume loss (μm m^3)		
Sample	25 °C	400 °C	750 °C	25 °C	400 °C	750 °C
850-2	0.399 ± 0.090	0.631 ± 0.094	0.716 ± 0.092	728 ± 6.54	819 ± 8.55	950 ± 9.85
850-4	0.439 ± 0.087	0.321 ± 0.086	0.593 ± 0.126	700 ± 7.82	649 ± 7.32	740 ± 6.55
850-6	0.326 ± 0.081	0.437 ± 0.082	0.512 ± 0.112	582 ± 4.54	600 ± 7.05	530 ± 7.04
900-2	0.323 ± 0.095	0.373 ± 0.091	0.443 ± 0.119	465 ± 4.58	549 ± 6.10	600 ± 6.46
950-4	0.375 ± 0.092	0.302 ± 0.073	0.532 ± 0.100	412 ± 4.24	530 ± 5.08	575 ± 6.88
950-6	0.280 ± 0.097	0.446 ± 0.135	0.515 ± 0.135	373 ± 3.54	415 ± 4.08	550 ± 5.55
1050-2	0.302 ± 0.084	0.308 ± 0.086	0.515 ± 0.091	334 ± 3.82	300 ± 3.92	500 ± 4.78
1050-4	0.328 ± 0.075	0.401 ± 0.145	0.413 ± 0.117	250 ± 5.20	286 ± 3.91	533 ± 6.02
1050-6	0.258 ± 0.084	0.398 ± 0.147	0.400 ± 0.074	228 ± 2.32	276 ± 2.96	498 ± 4.87
I-718	0.708 ± 0.097	0.797 ± 0.106	0.838 ± 0.174	1254 ± 9.87	2243 ± 12.05	3195 ± 14.07

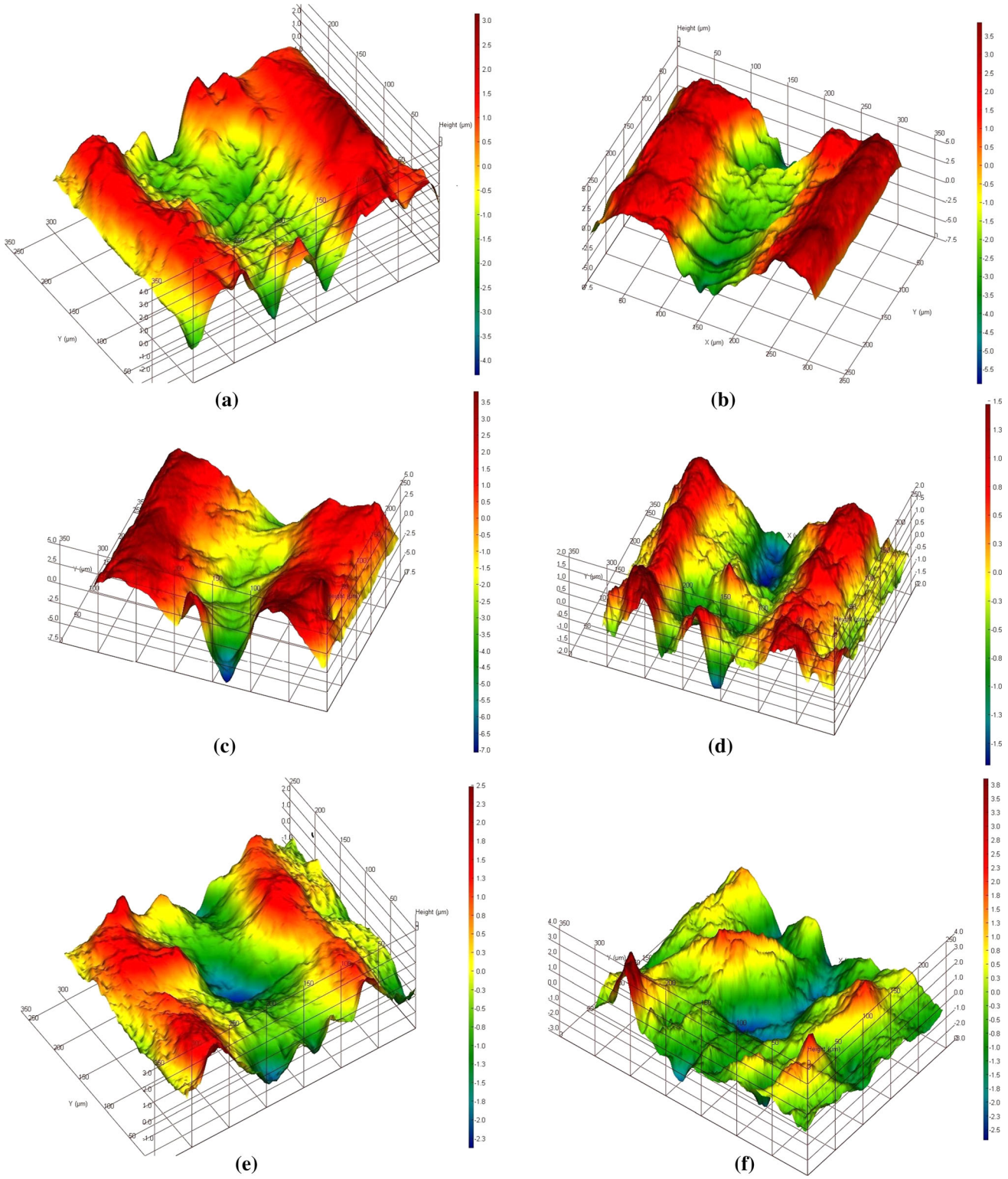

Fig. 7—3D wear traces and profiles of the untreated samples (I-718) subjected to wear testing at (*a*) 25 °C, (*b*) 400 °C, (*c*) 750 °C, and the least worn samples (1050-6) wear-tested at (*d*) 25 °C, (*e*) 400 °C, (*f*) 750 °C under 5 N loading.

untreated Inconel 718 is two-body abrasion, with cutting occurring at room temperature and plowing occurring at elevated temperatures.

When images of the worn surface of sample 850-2 (Figure 9) tested at 25 °C, 400 °C, and 750 °C are compared it can be seen that all three images display evidence of microcutting, microcracking and localized spalling. Note that the wear track is relatively smooth at room temperature, while deeper wear grooves are produced at 400 °C and 750 °C. Microcracks are

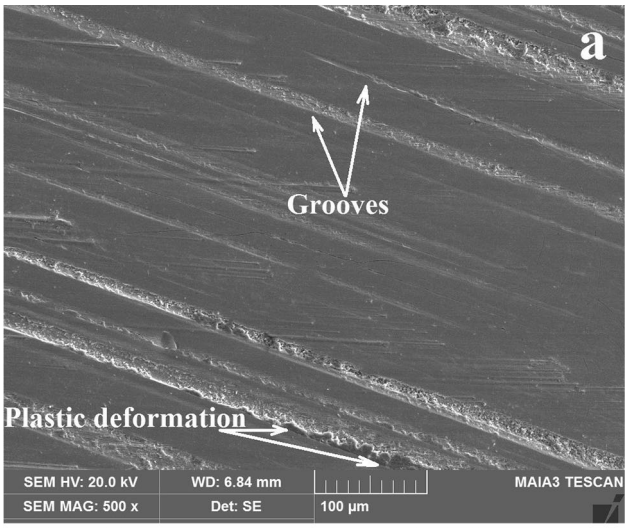

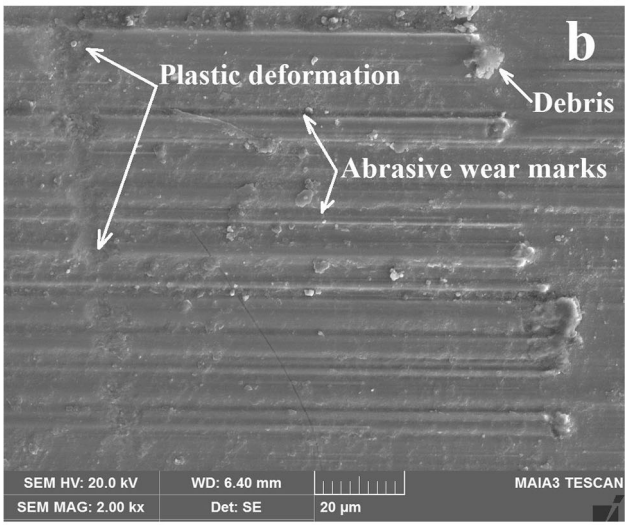

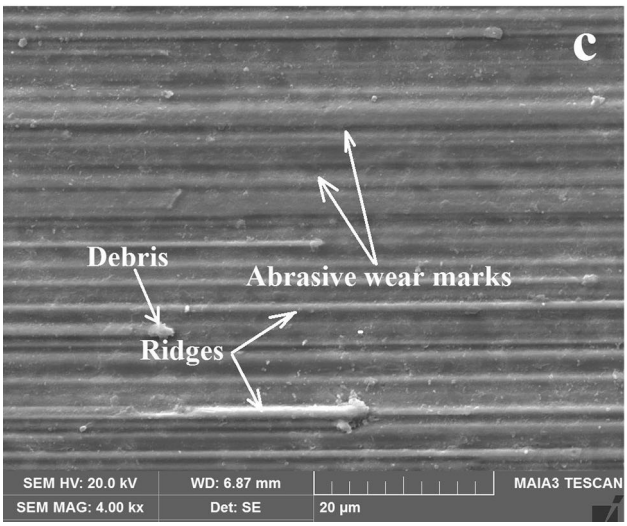

Fig. 8—SEM views obtained from untreated Inconel 718 after the wear experiments performed at the temperatures of (*a*) 25 °C, (*b*) 400 °C, and (*c*) 750 °C.

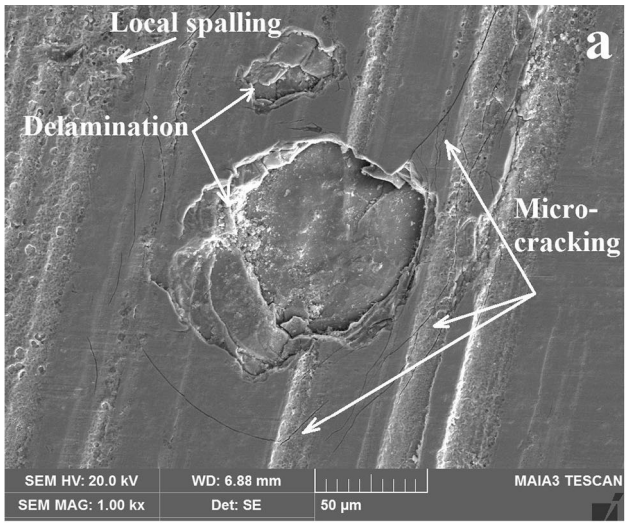

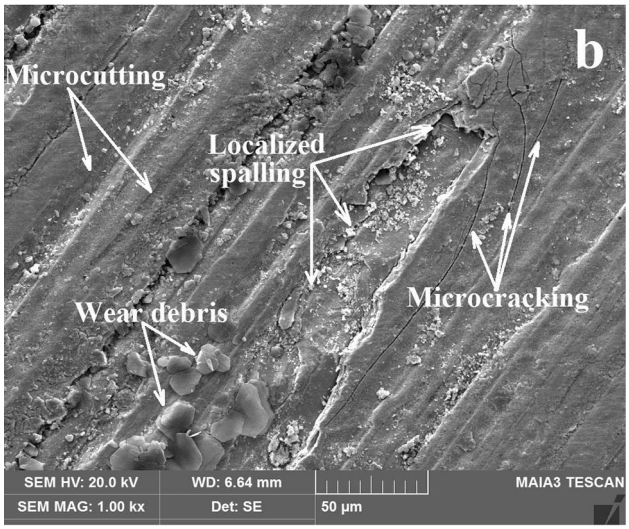

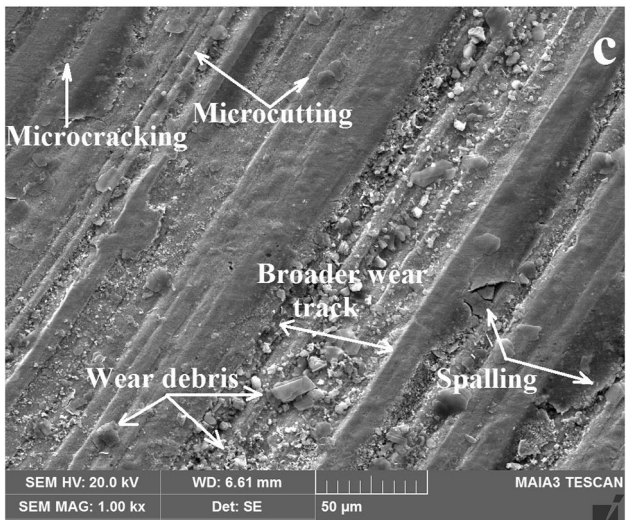

Fig. 9—SEM views obtained from 850-2 after the wear tests performed at the temperatures of (*a*) 25 °C, (*b*) 400 °C, and (*c*) 750 °C under 5 N load.

present in the boride coating for all three test temperatures. The different phases formed on the surface have different chemical compositions, thermal expansion coefficients, and mechanical behavior. These phases are separated during sliding by the applied load and delamination occurs.[32,34] Due to repetitive forces acting

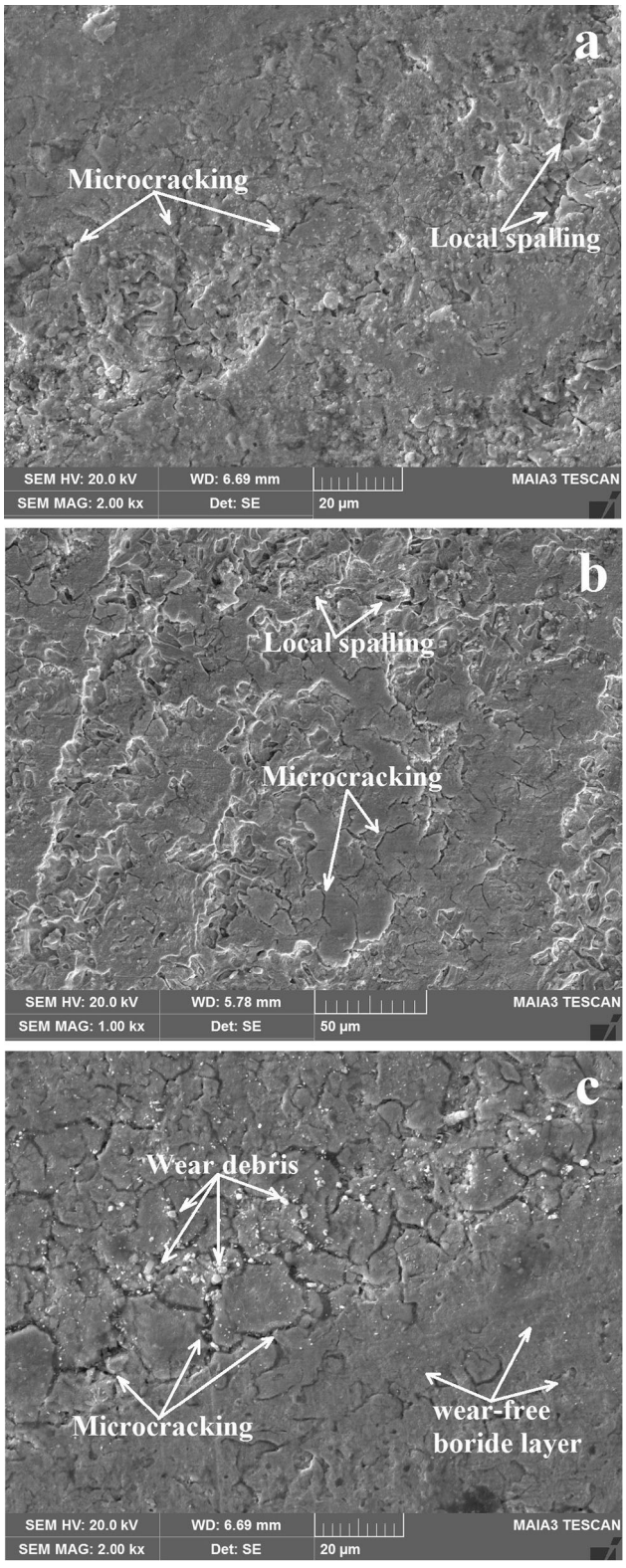

Fig. 10—SEM images obtained from S8 after the wear experiments carried out at the temperatures of (*a*) 25 °C, (*b*) 400 °C, and (*c*) 750 °C under 5 N load.

on surface asperities and wear debris microcracks develop beneath the surface, and eventually spalling occurs.[36] At room temperature, the wear marks are shallow (Figure 9(a)), but as the temperature is increased to 750 °C, the resulting wear grooves become broader and deeper, while the wear mechanism remains the same (Figure 9(c)).

The wear resistance of the samples increased and the wear mechanisms changed with increasing coating thickness. The wear surface of S8 shows indications of microcracking similar to that observed in 850-2, but microcutting is almost entirely absent, indicating three-body abrasion as the effective wear mechanism. During sliding some of the wear debris was expelled from the system while the rest was trapped and subjected to repeated loads between the abrasive ball and counterface. The debris produced under repeated loads possesses increased hardness, and either sinks into the abraded surface or enters between the abrasive ball and counterface; the latter leads to three-body abrasion.[34] Moreover, as the temperature is increased, the average size of the microcracks increase (Figures 10(b) and (c)), but there is no significant change in the wear mechanism.

The surface of the WC abrasive ball was also examined at the end of each of the wear tests (Figure 11), and compared with the changes measured in its weight.

The weight of the WC ball was 1.639 g at the beginning of the wear tests. Its weight was measured as 1.639 g (no change) after testing at room temperature, 1.641 g after testing at 400 °C (which was considered as a negligible change) and 1.895 g at after testing at 750 °C. The increased weight of the ball after testing at 750 °C indicated the possibility of adhesion from the coating layer. SEM images of the surface of the WC ball used in the room temperature (Figure 11(a)) and 250 °C (Figure 11(b)) wear tests reveal evidence of microcutting and pitting. The ball used in the 750 °C tests, on the other hand (Figure 11(c)), shows signs of localized adhesive transfer (marked as Spot 3 and Spot 4). EDS analyses were carried out on the surface of the ball (Figure 11(c)) to identify the chemistry of the adhering material, which revealed high amounts of Cr, Ni, Fe, O, and B. Results of the EDS analyses and the weight increase in the WC abrasive ball therefore suggest that some of the oxides produced during wear testing at 750 °C were transferred onto the surface of the WC ball. The fact that the WC ball displayed minimal wear despite having a hardness was lower than the borided surfaces can be explained as due to the high roughness of the coating layer,[11] it is probable that a significant amount of coating removal occurred during wear testing from the fracture of asperities. As a result, the rough material with greater hardness tends to wear more rapidly than the smoother surface with the smaller modulus.[37]

IV. CONCLUSION

In the present study, the surface of Ni-based Inconel 718 superalloy was boronized with a nano-sized blend of 90 wt pct B_4C and 10 wt pct $NaBF_4$ powders using the pack-boronizing technique at the temperatures of

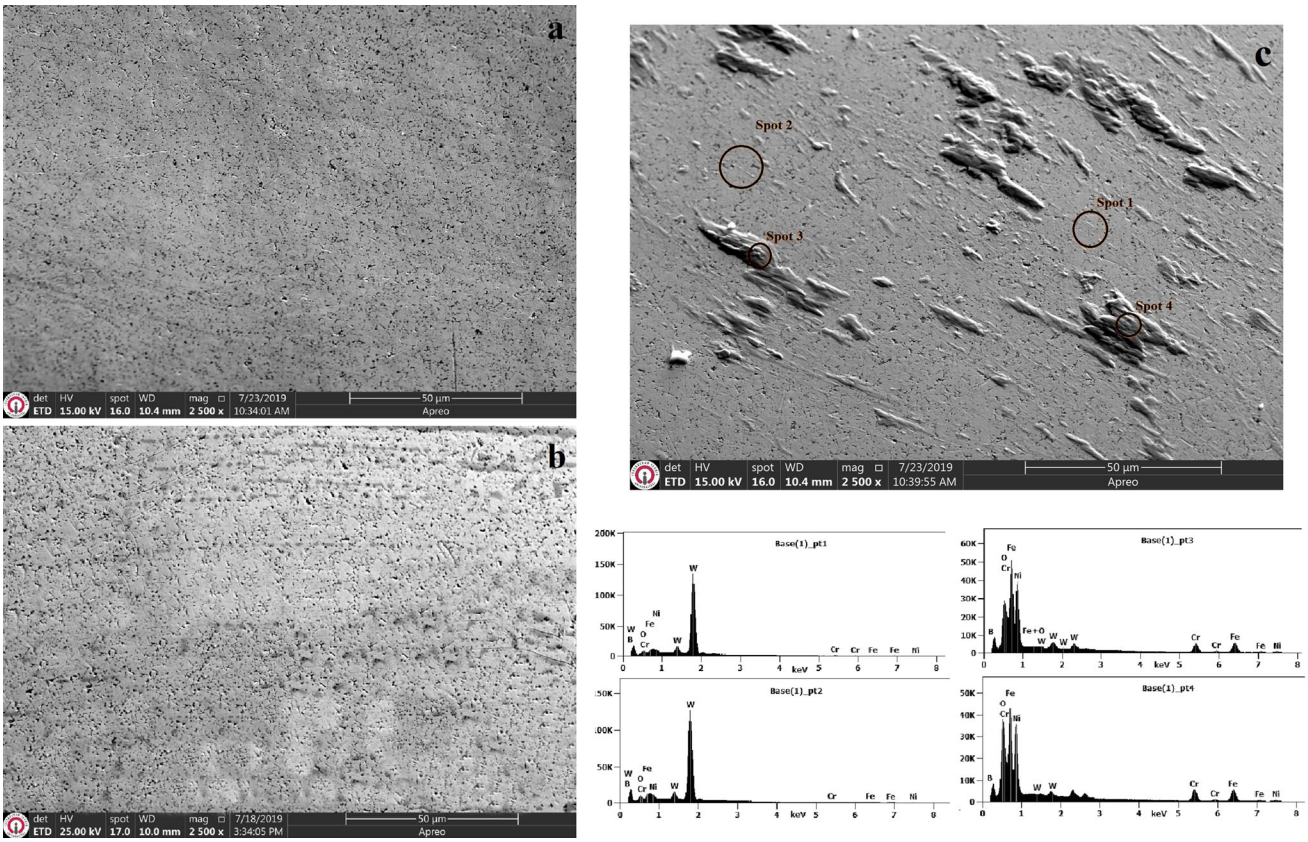

Fig. 11—SEM images obtained from the surface of the WC ball after wear tests performed at the temperatures of (*a*) 25 °C, (*b*) 400 °C, and (*c*) 750 °C under 5 N load.

850 °C, 950 °C, and 1050 °C for 2, 4, and 6 hour. The untreated and boronized samples were subjected to wear testing at 25 °C, 400 °C, and 750 °C. The obtained results are summarized as follows:

1. Silicide-free boride layers were successfully grown on Inconel 718 Ni-based superalloy surface by the powder pack-boronizing process using nano-sized B_4C powder.
2. A double-phase boride layer with a distinct boundary separating the outer and inner phase was formed at 850 °C and 950 °C while a complex multi-phase boride layer was formed at 1050 °C.
3. Increase in boronizing temperature and time resulted in increased thickness, hardness, and surface roughness values of the boride layers.
4. XRD analyses revealed that the predominant phases in the boride coating were Ni_3B_4, Cr_2B and minor amounts of Cr_3Ni_2, Cr_2B_3, FeB, and Fe_2B.
5. The increase in surface hardness achieved by the boronizing process resulted in boronized samples exhibiting COF values lower than the untreated alloy. The COF values of all samples increased with increasing temperature.
6. All of the boronized samples displayed superior wear resistance compared to the untreated sample under all wear-test conditions. Wear resistance increased with the increasing hardness and decreased with the increasing wear-test temperature.
7. The effective wear mechanism in the untreated Inconel 718 was microcutting and plowing, with microcutting occurring at room temperature and plowing occurring at elevated temperatures. In the boronized samples, microcutting was observed only where thin boride coatings were present. Regardless of the wear-test temperature, the effective wear mechanism was oxidative wear assisted by microcracking and spalling. When the thickness of the boride layer was increased by increasing the boronizing temperature/time, a transition from two-body to three-body abrasion was observed in the wear tests.
8. The WC abrasive ball did not suffer any wear loss in the experiments carried out at room temperature and 250 °C. However, in the experiments carried out at 750 °C, the weight of the ball increased due to adhesion from the surfaces of the wear-test specimens.
9. Boronized Inconel 718 was capable of sustaining its coating under 5 N for 1800 m at temperatures up to 750 °C.
10. The results of this study have shown that the wear resistance of Inconel 718 can be improved by the pack-boronizing process. The wear behavior of borided superalloys in corrosive liquids remains to be investigated in future studies.

REFERENCES

1. H. Zhang, C. Li, Q. Guo, Z. Ma, Y. Huang, H. Li, and Y. Liu: *Mat. Sci. Eng. A*, 2018, vol. 722, pp. 136–46, https://doi.org/10.1016/j.msea.2018.02.093.
2. A. Thomas, M. El-Wahabi, J.M. Cabrera, and J.M. Prado: *J. Mater. Process. Tech.*, 2006, vol. 177, pp. 469–72, https://doi.org/10.1016/j.jmatprotec.2006.04.072.
3. S. Kumar, G.S. Rao, K. Chattopadhyay, G.S. Mahobia, N.C.S. Srinivas, and V. Singh: *Mater. Design.*, 2014, vol. 62, pp. 76–82, https://doi.org/10.1016/j.matdes.2014.04.084.
4. A.D. Sharma, A.K. Sharma, and N. Thakur: *J. Alloy. Compd.*, 2014, vol. 597, pp. 175–80, https://doi.org/10.1016/j.jallcom.2014.02.011.
5. M.M. Ma, Z.M. Wang, and X.Y. Zeng: *Mater. Charact.*, 2015, vol. 106, pp. 420–27, https://doi.org/10.1016/j.matchar.2015.06.027.
6. T. Kurzynowski, I. Smolina, K. Kobiela, B. Kuźnicka, and E. Chlebus: *Mater. Design.*, 2017, vol. 132, pp. 349–59, https://doi.org/10.1016/j.matdes.2017.07.024.
7. H. Dinc, A. Motellabzadeh, M. Baydogan, and H. Cimenoglu: *Acad. J. Sci.*, 2013, vol. 2 (2), pp. 385–89.
8. A. Günen, E. Kanca, H. Çakir, M.S. Karakaş, M.S. Gök, Y. Küçük, and M. Demir: *Surf. Coat. Tech.*, 2017, vol. 311, pp. 374–82, https://doi.org/10.1016/j.surfcoat.2016.12.097.
9. A. Günen and E. Kanca: *Materia*, 2017, vol. 22, p. 2, https://doi.org/10.1590/s1517-707620170002.0161.
10. M. Aghaie-Khafri and M. Mohamadpour Nazar Abady: *JOM*, 2012, vol. 64 (6), pp. 694–701, https://doi.org/10.1007/s11837-012.
11. A. Günen, E. Kanca, M.S. Karakaş, V. Koç, M.S. Gök, Y. Kanca, and M. Demir: *Surf. Coat. Tech.*, 2018, vol. 348, pp. 130–41, https://doi.org/10.1016/j.surfcoat.2018.04.071.
12. T. Arai:The thermo-reactive deposition and diffusion process for coating steels to improve wear resistance in *Thermochemical Surface Engineering of Steels*, E.J. Mittemeijer and M.A.J. Somers, eds., Elsevier, Amsterdam, 2015. 10.1533/9780857096524.5.703.
13. F. Czerwinski, Thermochemical treatment of metals. In Heat Treatment-Conventional and Novel Applications. InTech. (2012) https://doi.org/10.5772/51566.
14. X.L. Xu, Z.W. Yu, and L.Y. Cui: Mater*Charact*, 2019, https://doi.org/10.1016/j.matchar.2019.109798.
15. H.J. Hunger and G. Trute: Succesful boronizing of nickel based alloys*Mater. Sci. Forum*, 1994, vols. 163–165, pp. 341–48.
16. W. Muhammad, K. Hussain, A. Tauqir, A. Ulhaq, and A.Q. Khan: *Metall. Mater. Trans. A*, 1999, vol. 30A, pp. 670–74, https://doi.org/10.1007/s11661-999-0059-z.
17. D.W. Deng, C.G. Wang, Q.Q. Liu, and T.T. Niu: Nonferr*Metal Soc.*, 2015, vol. 25 (2), pp. 437–43, https://doi.org/10.1016/S1003-6326(15)63621-4.
18. A. Günen and E. Kanca: Pamukkale University*J. Eng. Sci.*, 2017, vol. 23 (4), pp. 411–16, https://doi.org/10.5505/pajes.2017.56689.
19. R.S. Petrova, N. Suwattananont, and V. Samardzic: *J. Mater. Eng. Perform.*, 2008, vol. 17 (3), pp. 340–45, https://doi.org/10.1007/s11665-008-9228-2.
20. I. Campos-Silva, A.D. Contla-Pacheco, A. Ruiz-Rios, J. Martínez-Trinidad, G. Rodríguez-Castro, A. Meneses-Amador, and W.D. Wong-Angel: *Surf. Coat. Tech.*, 2018, vol. 349, pp. 917–27, https://doi.org/10.1016/j.surfcoat.2018.05.086.
21. K.M. Doleker, O. Odabas, Y. Ozgurluk, K. Asgarov, and A.C. Karaoglanli: *Mater. Res. Exp.*, 2019, https://doi.org/10.1088/2053-1591/ab26d8.
22. S. Kumar, B. Satapathy, D. Pradhan, and G.S. Mahobia: *Mater. Res. Exp.*, 2019, vol. 6, p. 8, https://doi.org/10.1088/2053-1591/ab1dc7.
23. K. Feng, Y. Chen, P. Deng, Y. Li, H. Zhao, F. Lu, R. Li, and Z. Li: *J. Mater. Process. Techn.*, 2017, vol. 243, pp. 82–91, https://doi.org/10.1016/j.jmatprotec.2016.12.001.
24. Y. Birol: *Wear*, 2010, vol. 269 (9–10), pp. 664–71.
25. O. Azouani, M. Keddam, A. Brahimi, and A. Sehisseh: *J. Min. Metall. Sect. B*, 2015, vol. 51 (1), pp. 49–54.
26. A. Günen, M. Ulutan, M.S. Gok, B. Kurt, and N. Orhan: *J. Balk. Tribol. Assoc.*, 2014, vol. 20 (3), pp. 362–79.
27. O. Ozdemir, M.A. Omar, M. Usta, S. Zeytin, C. Bindal, and A.H. Ucisik: *Vacuum*, 2008, vol. 83 (1), pp. 175–79, https://doi.org/10.1016/j.vacuum.2008.03.026.
28. M.S. Karakaş, A. Günen, E. Kanca, and E. Yilmaz: *Arch. Metall. Mater.*, 2018, vol. 63 (1), pp. 159–65, https://doi.org/10.24425/118923.
29. K.G. Thirugnanasambantham, R. Raju, T. Sankaramoorthy, P. Velmurugan, A. Kannagi, M. Chaitanya, K. Reddy, V.S. Koushik Chary, M.A. Mustafa, and V. Ramesh Chandra: *Cogent Eng*, 2018, vol. 5 (1), p. 1501864, https://doi.org/10.1080/23311916.2018.1501864.
30. H.L. Du, P.K. Datta, I.A. Inman, R. Geurts, and C. Kubel: *Mat. Sci. Eng. A*, 2003, vol. 357, pp. 412–22, https://doi.org/10.1016/S0921-5093(03)00258-2.
31. M.S. Gök, Y. Küçük, A. Erdoğan, M. Öge, E. Kanca, and A. Günen: *Surf. Coat. Tech.*, 2017, vol. 328, pp. 54–62, https://doi.org/10.1016/j.surfcoat.2017.08.008.
32. C. Zimmerman: *Boriding (Boronizing) of Metals, ASM Handbook, Heat Treating*, ASM International, Cleveland, 2013, pp. 709–24. https://doi.org/10.31399/asm.hb.v04a.a0005772.
33. J.C.A. Batista, A. Matthews, and C. Godoy: *Surf. Coat. Tech.*, 2001, vols. 142–144, pp. 1137–43, https://doi.org/10.1016/S0257-8972(01)01189-6.
34. B. Kurt, Y. Küçük, and M.S. Gök: *Tribol. T.*, 2014, vol. 57 (2), pp. 345–52.
35. A. Günen, B. Kurt, P. Milner, and M.S. Gök: *Int. J. Ref. Met. Hard Mater.*, 2019, vol. 81, pp. 333–44, https://doi.org/10.1016/j.ijrmhm.2019.03.019.
36. A. Pauschitz, M. Roy, and F. Franek: *Tribol. Int.*, 2008, vol. 41 (7), pp. 584–602, https://doi.org/10.1016/j.triboint.2007.10.003.
37. B.L. Strahin, D.D. Shreeram, and G.L. Doll: *JOM.*, 2017, vol. 69 (7), pp. 1160–64, https://doi.org/10.1007/s11837-017-2370-2.